



POLİTEKNİK DERGİSİ

JOURNAL of POLYTECHNIC

ISSN: 1302-0900 (PRINT), ISSN: 2147-9429 (ONLINE)

URL: <http://dergipark.org.tr/politeknik>



Investigation of the effects of axle load on tyre behaviour in vehicles

Taşıtlarda aks yükünün lastik davranışına etkilerinin incelenmesi

Yazar(lar) (Author(s)): Turan Alp ARSLAN¹, İbrahim ÇELİK², Faruk Emre AYSAL³, Hüseyin BAYRAKÇEKEN³

ORCID¹: 0000-0003-3259-4854

ORCID²: 0000-0002-8857-1910

ORCID³: 0000-0002-9514-1425

ORCID⁴: 0000-0002-1572-4859

To cite to this article: Arslan T. A., Çelik İ., Aysal F. E. ve Bayrakçeken H., “Investigation of the effects of axle load on tyre behaviour in vehicles”, *Journal of Polytechnic*, 27(2): 603-614, (2024).

Bu makaleye şu şekilde atıfta bulunabilirsiniz: Arslan T. A., Çelik İ., Aysal F. E. ve Bayrakçeken H., “Investigation of the effects of axle load on tyre behaviour in vehicles”, *Politeknik Dergisi*, 27(2): 603-614, (2024).

Erişim linki (To link to this article): <http://dergipark.org.tr/politeknik/archive>

DOI: 10.2339/politeknik.1187066

Investigation of the Effects of Axle Load on Tyre Behaviour in Vehicles

Highlights

- ❖ The effects of axle load variation on important parameters of vehicle tyre mechanics such as slip angle, lateral force, self-aligning torque, and camber thrust were investigated.
- ❖ The mathematical model based on the Fiala tyre model was verified.

Graphical Abstract

In this study, the effect of axle load on important parameters of tyre mechanics and tyre behaviour in vehicles was investigated mathematically.

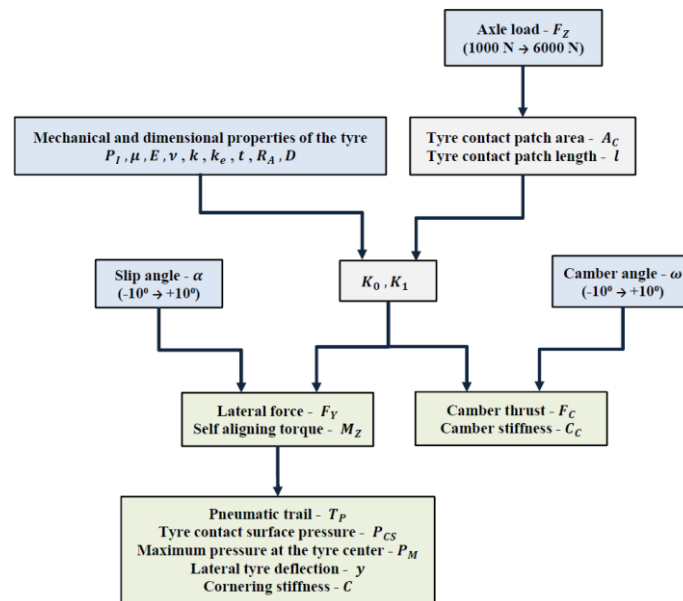


Figure. The flow chart of the mathematical model

Aim

It was aimed to examine in detail the effect of axle load change on tyre behaviour in vehicles.

Design & Methodology

The study was carried out with the mathematical model based on the Fiala tyre model. A single-wheel sample with a standard 205/55R16 pneumatic tyre was investigated in terms of flexible wheel-rigid ground road interaction under dry asphalt road conditions.

Originality

The dynamic load distribution on vehicle axles is constantly changing for some reasons such as braking, acceleration, and road slope. The force, torque, and slip values observed in each wheel are different from each other. With the model presented in the study, it is possible to obtain information about the behaviour of the tyres moving parallel to each other, as well as the front or rear axle.

Findings

For axle load values, significant parameters such as slip angle, lateral force, self-aligning torque and camber thrust, as well as pneumatic trail, tyre contact area pressure distribution, lateral tyre deflection, cornering stiffness and camber stiffness were determined.

Conclusion

Tyre behaviour in vehicles is greatly affected by the axle load as well as tyre mechanical properties and tyre dimensional properties.

Declaration of Ethical Standards

The authors of this article declare that the materials and methods used in this study do not require ethical committee permission and/or legal-special permission

Investigation of the Effects of Axle Load on Tyre Behaviour in Vehicles

Araştırma Makalesi / Research Article

Turan Alp Arslan^{1*}, İbrahim Çelik², Faruk Emre Aysal², Hüseyin Bayrakçıken¹

¹ Afyon Kocatepe University, Faculty of Technology, Department of Automotive Engineering, Afyon, Türkiye

² Afyon Kocatepe University, Faculty of Technology, Department of Mechatronics Engineering, Afyon, Turkey

(Geliş/Received : 10.10.2022 ; Kabul/Accepted : 02.11.2022 ; Erken Görünüm/Early View : 27.11.2022)

ABSTRACT

In this study, the slip angle which is a significant parameter in the operation of vehicle safety and control systems was investigated mathematically. With the model developed based on the Fiala tire model, the variation of the lateral force and self-aligning torque depending on the slip angle was obtained for the axle load values between 1000 N and 6000 N. By using these parameters, pneumatic trail, tyre contact area pressure distribution, tyre contact area maximum pressure value, lateral tyre deflection, and cornering stiffness were calculated. Similarly, for certain values of camber angle, camber thrust, and camber stiffness were examined. The changes of all these parameters which are of great importance for tyre mechanics depending on the axle load was investigated. A single-wheel sample with a standard 205/55R16 pneumatic tyre was investigated in terms of flexible wheel-rigid ground road interaction under dry asphalt road conditions..

Keywords: Axle loads, tyre mechanics, slip angle, lateral force, vehicle dynamics.

Taşıtlarda Aks Yükünün Lastik Davranışına Etkilerinin İncelenmesi

ÖZ

Bu çalışmada, taşıt güvenlik ve kontrol sistemlerinin işletilmesinde önemli bir parametre olan kayma açısı matematiksel olarak incelenmiştir. Fiala lastik modeli temel alınarak oluşturulan matematiksel model ile aks yükünün 1000 N ile 6000 N arasındaki değerleri için yanıl kuvvet ve kendini ayarlama torkunun kayma açısına bağlı değişimi belirlenmiştir. Bu parametreler ile pnömatrik iz mesafesi, temas alanı basınç dağılımı, temas alanı maksimum basınç değeri, yanıl lastik sapması ve viraj rijitliği değeri hesaplanmıştır. Benzer şekilde kamber açısının belirli değeri için ise kamber itki kuvveti ve kamber rijitliği değeri incelenmiştir. Lastik mekaniği için büyük önem arz eden tüm bu parametrelerin aks yüküne bağlı olarak değişimleri araştırılmıştır. Çalışmada 205/55R16 ebatlarındaki standart bir pnömatrik lastiğe sahip tek bir tekerlek örneği, kuru asfalt yol şartlarında, esnek tekerlek-rijit zemin yol etkileşimi açısından araştırılmıştır.

Anahtar Kelimeler: Aks yükü, lastik mekaniği, kayma açısı, yanıl kuvvet, taşıt dinamiği.

1. INTRODUCTION

Deaths and injuries resulting from traffic accidents are an important problem globally. The number of deaths in traffic accidents around the world increased rapidly from 2000 to 2018, rising from 1.15 million to 1.35 million. Therefore, approximately 2.37% of the 56.9 million deaths worldwide are caused by traffic accidents [1,2]. For this reason, studies on the prevention of traffic accidents continue increasingly [3-6]. The development of vehicle safety systems is at the forefront of efforts to prevent traffic accidents. In the past few decades, various vehicle safety systems have been developed to improve vehicle and passenger safety. These systems try to prevent undesirable vehicle behaviour through the active vehicle control. Thus, it helps drivers to maintain vehicle control more safely and comfortably. ABS, ESC, and TCS are the leading vehicle safety systems used in today's vehicles [7-10].

ESC, an important vehicle safety system, was developed and started to be used in the early 1990s. The ESC system has been developed to increase vehicle stability by using the distribution of braking forces [11,12]. Thus, vehicle safety is increased by improving driving stability. For this reason, the ESC system has been used as a basic feature in all vehicles since the late 2000s [13,14]. In general, ESC is a system that ensures vehicle stability by observing vehicle conditions and driver inputs in real time. Many sensors are needed for this purpose in vehicles. However, the least possible number of sensors are used in vehicles in order to reduce costs. Therefore, reducing the number of sensors has become one of the important issues in studies on ESC. Stability in vehicle dynamics can be achieved by determining the slip angle and lateral forces. These two parameters are of great importance in the control of the ESC system. Additionally, there is a direct relationship between the slip angle value of the vehicle tyre and the lateral forces generated in the tyre. This situation has led to an increase in studies on the slip angle. It is seen that model observer

*Sorumlu Yazar (Corresponding Author)
e-posta : talparslan@aku.edu.tr

methods such as Kalman Filter and Luenbenger [15-17], full vehicle experiments using GPS or driver recorder [18-20], finite element method or some simulation software such as CarSim and MATLAB Simulink [21-23] and tyre models such as Magic Formula are used extensively in vehicle slip angle estimation [24,25].

Various studies have been carried out by developing many different approaches to the accurate determination of the slip angle. In the literature, basically three approaches are used to estimate the slip angle or its effect on the vehicle. The first method is to use the data provided by the lateral slip velocity sensor in the ESC system instead of the slip angle. However, it is known that the prediction performance is affected by the errors caused by the deviations of the sensors, road slope, and bank angle [15]. The second approach which designs the sensors to predict slip angle needs accurate information about vehicle speed, road friction coefficient, and some tyre parameters that need to be measured directly. Although this approach has difficulties in data collection, it provides the most accurate result if the data can be obtained correctly, since the method is directly based on analytical modelling [14-17].

The third method is to estimate the slip angle with the help of measurements of systems such as GNSS and GPS. For this purpose, a combination of GPS and INS has been used to estimate the lateral slip angle accurately [26]. In other studies, data provided by components such as wheel force converters, optical encoders and IMU, and GPS data are processed together to create systems that perform slip angle estimations [27-31]. However, satellite signals are extremely sensitive to changes in the environment and weather. Therefore, the GPS data is not always reliable enough. This situation creates a significant disadvantage for the third method. If the vehicle's general condition in motion can be accurately determined, systems that are more sensitive than the other two methods can be designed with the second method to estimate the slip angle. Therefore, many studies have been conducted on estimating nonlinear wheel forces [32-35] and developing new methods for slip angle estimation in order to solve this problem effectively [36-39].

In this study, slip angle which is an significant parameter in the operation of vehicle safety and control systems such as ESC was mathematically investigated. In other words, the analytical approach which is the second method in the literature was taken as a basis for determining the slip angle. Based on the Fiala tyre model, the lateral force and self-aligning torque values were determined for certain values of the slip angle. Using these values, pneumatic trail, tyre contact area pressure distribution, maximum pressure value at the center of tyre contact surface, lateral tyre deflection, and cornering stiffness were obtained. Similarly, camber thrust and camber stiffness were investigated for certain values of camber angle. The changes of all these parameters which are of great importance for tyre mechanics depending on the axle load were investigated. The dynamic load

distribution on vehicle axles is constantly changing due to some reasons such as braking, acceleration, and road slope [40]. Therefore the force, torque, and slip values observed in each wheel are different from each other. With the model presented in the study, it is possible to obtain information about the behaviour of the tyres moving parallel to each other, as well as the front or rear axle

2. TYRE MECHANICS

2.1 Slip Angle and Camber Thrust

Under normal conditions, when a vehicle is moving in a straight direction, the wheel moves in a plane coincident with the direction of travel. In this case, a lateral force acting on the wheel does not arise. However, in case of lateral movement of the vehicle, the direction of movement is unaligned with the plane of rotation. As seen in Figure 1, this angle between the wheel's direction of travel and the plane of rotation in the case of lateral movement is called the slip angle [7,41]. Additionally, the lateral force acting on the wheel during rotation creates a lateral holding force on the tyre contact patch. It is desired that the lateral force acting on the lateral moving wheel be as large as possible considering the independent movement of the vehicle, the steering effects, and the reaction of the vehicle [42,43]. The forces acting on the wheel are constantly changing along the tyre contact patch between the tyre and the road. A tyre in lateral motion is deformed from the tyre contact patch and its outer circumference as shown in Figure 1. While this deformation in the tyre causes a change in the contact patch, it also causes the movement of the lateral force along this surface [44]. The lateral force generated during deformation is not on the same axis as the center of the contact patch. Therefore, the lateral force produces a moment called self-aligning torque at the center of the tire contact patch [7,45]. This torque occurs in the direction that reduces the slip angle of the tyre. The distance between the point where the lateral force acts on the contact patch and the vertical tyre axis is the pneumatic trail. The distance between the rotation axis and the points where the vertical tyre axes coincide with the ground is the mechanical trail [46].

The angle between the wheel center axis and the vertical axis is the camber angle. The wheel center axis is the axis passing through the center of the wheel. The vertical axis is the axis perpendicular to the ground. In positive camber, the upper part of the wheels appears more outward compared to the lower part and is further away from the vehicle body. On the other hand, in negative camber, the upper part of the wheels appears more inward than the lower part and is closer to the vehicle body [47].

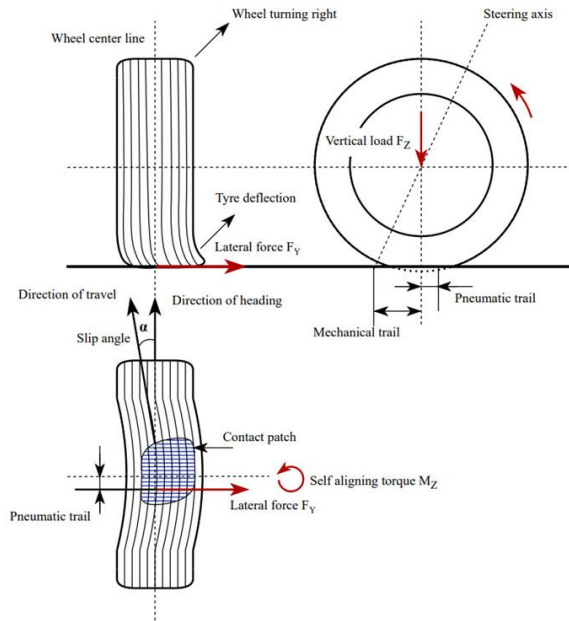


Figure 1. Slip angle and tyre deflection

Figure 2 shows a wheel with a negative camber angle. With the appropriate camber angle, it is aimed to minimize the mechanical loads on the wheel alignment and suspension parts, to provide smooth tyre wear, to improve road holding, and to provide ease of turning [43]. In a free movement of a wheel with a camber angle, the contact patch follows a central circular path. However, when the tyre is forced to move in a straight direction, shear stress occurs between the tread rubber and the road, and deformation is observed in the tyre. A lateral force causing this deformation acts on the contact patch as seen in Figure 2. This second source of lateral force acting on the tyre is called camber thrust [42,48]. The camber thrust is observed in the direction of the tyre's slope.

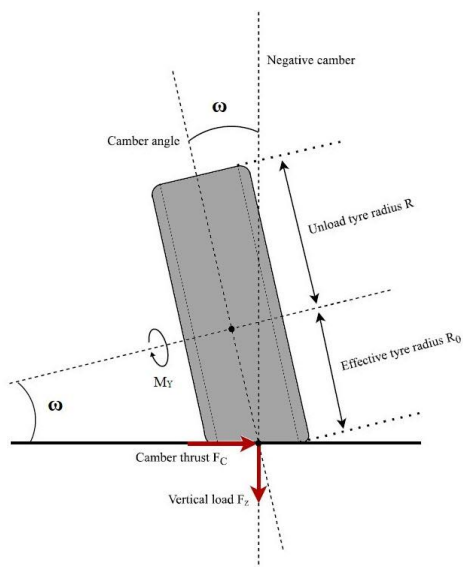


Figure 2. Camber angle and camber thrust

As seen in Figure 2, a negative camber angle creates a negative camber thrust for the wheel [49]. For this reason, with the negative camber angle, the lateral and cornering forces of the tyre are increased and the camber thrust force is utilized in the best way [45]. Especially in front-wheel drive vehicles, it is desirable for the rear wheels to increase the negative camber angle according to the amount of vehicle rotation. This is not useful as it will cause problems in transferring the traction power to the ground at the drive wheels [48].

2.2 Tyre Structural Model

The magic formula, FEM, and Fiala tyre models are the main tyre models developed until today [50]. In this study, the Fiala tyre model was used to examine the effects of axle load on tyre dynamics. This model, introduced by Fiala [51], provides a basis for a full vehicle model and tyre simulation. Additionally, this model is one of the widely accepted theories in the analysis of slip angle, lateral force, self-aligning torque, and camber thrust with its easy-to-understand structure [52]. As seen in Figure 3, Fiala's structural tyre model consists of four different parts. These parts are a rigid body equivalent to a rim, an elastically deformable sidewall in both the lateral and vertical directions, a thin steel belt connecting the sidewalls, and a tread rubber. According to this model, the tyre consists of many independent springs around it and is not circular at all points. While the lateral force F_y acting on the contact point and the vertical force F_z , called the axle load, cause deforming tyre, the rigid rim is not deformed. The tread rubber and the sidewall are subjected to bending deformation in the lateral and vertical directions due to these forces. At the same time, the shear force between the ground surface and the tread rubber also affects the deformation of the tyre [42].

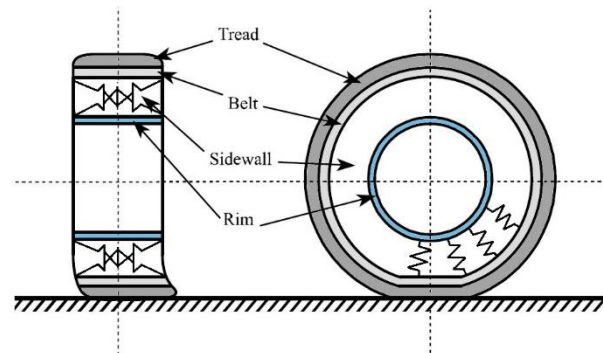


Figure 3. Tyre structural model [42]

3. MATERIAL AND METHOD

With the model created based on the Fiala tyre model, a lot of information about tyre dynamics can be obtained using a limited number of input parameters. The input parameters shown in Table 1 are directly related to the mechanical properties and basic dimensions of the tyre. Tyre's basic dimensions are shown in Figure 4

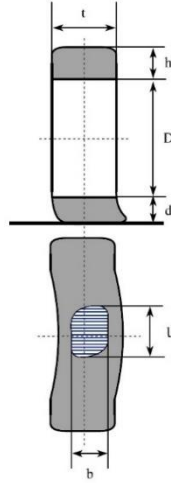


Figure 4. Basic dimensions of the tyre

The parameters shown in Table 1 for real tyre models can be determined by simple measurements. By combining the slip behaviour of the tyre in force and moment calculations, a more realistic version of the combined slip can be obtained. In addition to these advantages, simplifications have been made in the model, such as the rectangular tyre contact area and the uniform distribution of the contact area forces.

Table 1. Input parameters and assumptions

Properties	Value
F_Z (N)	1000 → 6000
k (kN/m)	820
k_e (kN/m)	190
E (MPa)	10
P_1 (kPa)	220,632
α (°)	-10 → +10
ω (°)	-10 → +10
$t/R_A/D$	205/55R16
μ	0,85
ν	0,499
d	0,9 · h
b	0,625 · t
Contact patch shape	Rectangle

The flow chart of the mathematical model of the study is shown in Figure 5. In the flow chart, blue blocks are input parameters, gray blocks are intermediate parameters and green blocks are output parameters. In vehicle dynamics, MATLAB Simulink software is used in many areas, from body behavior such as slip and roll over to suspension models [53,54]. In this study, in which the effects of axle load on tyre mechanics were investigated, important parameters of tyre mechanics were investigated for the values of axle load between 1000 N and 6000 N using the MATLAB Simulink software. First of all, tyre contact area and contact length were determined for these axle loads, and K_0 and K_1 values were calculated using the input parameters and assumptions given in Table 1. In the next step, lateral force and self-aligning torque values were determined for slip angle values between -10° and +10°. By using these values, pneumatic trail, tyre contact

patch pressure distribution, maximum pressure value in the tyre contact patch center, lateral tyre deflection, and cornering stiffness were obtained. Similarly, the camber thrust and camber stiffness were examined for the values of the camber angle between -10° and +10°. A single-wheel sample with a standard 205/55R16 pneumatic tyre was investigated in terms of flexible wheel-rigid ground road interaction under dry asphalt road conditions.

Tyre contact area A_c and contact length l are of great importance in determining the lateral force F_Y , self-aligning torque M_Z , slip angle α , and camber thrust F_C values [44,55]. In the study where the contact area is considered to be rectangular and the tyre tread structure is not taken into account these parameters are determined as follows. Here, A_c is the tyre contact area, F_Z is the vertical load, also called the axle load, b is the tyre contact area width, l is the tyre contact area length, and t is the tyre width. In the created model, the cases where the ratio of tyre contact area width to tyre width is between 0.55 and 0.70 were examined. As an example, the width of the tyre contact area is assumed to be 0.625 of the tyre width.

$$A_c = \frac{F_Z}{P_1} = b \cdot l \tag{1}$$

$$b = 0,625 \cdot t \tag{2}$$

After determining the tyre contact area and contact length, the calculated K_0 and K_1 values are expressed as follows [42]. Here k is the spring constant per unit length, G is the shear modulus of the tread rubber, E is Young's modulus of the tread rubber, d is the tyre sidewall height during deformation, ν is the poisson's ratio of the tread rubber, I is the moment of inertia of the contact surface area, h is the tyre sidewall height, and R_A is the tyre section ratio. In this study, cases where the ratio of the deformed tyre sidewall height to the tyre sidewall height is between 0.85 and 0.95 were examined. As an example, the deformed tyre sidewall height is assumed to be 0.90 of the tyre sidewall height. Tyre sidewall height is calculated using tyre width and section ratio values

$$K_1 = \frac{K_0}{1 + \frac{\beta^3 \cdot l^3}{12 \cdot k} \cdot K_0} \tag{3}$$

$$K_0 = G \cdot \frac{b}{d} = \frac{E}{2 \cdot (1 + \nu)} \cdot \frac{b}{d} \tag{4}$$

$$\beta = \frac{1}{\sqrt{2}} \cdot \left(\frac{k}{E \cdot I} \right)^{\frac{1}{4}} \tag{5}$$

$$I = \frac{l \cdot b^3}{12} \tag{6}$$

$$d = 0,9 \cdot h \tag{7}$$

$$h = \frac{R_A \cdot t}{100} \tag{8}$$

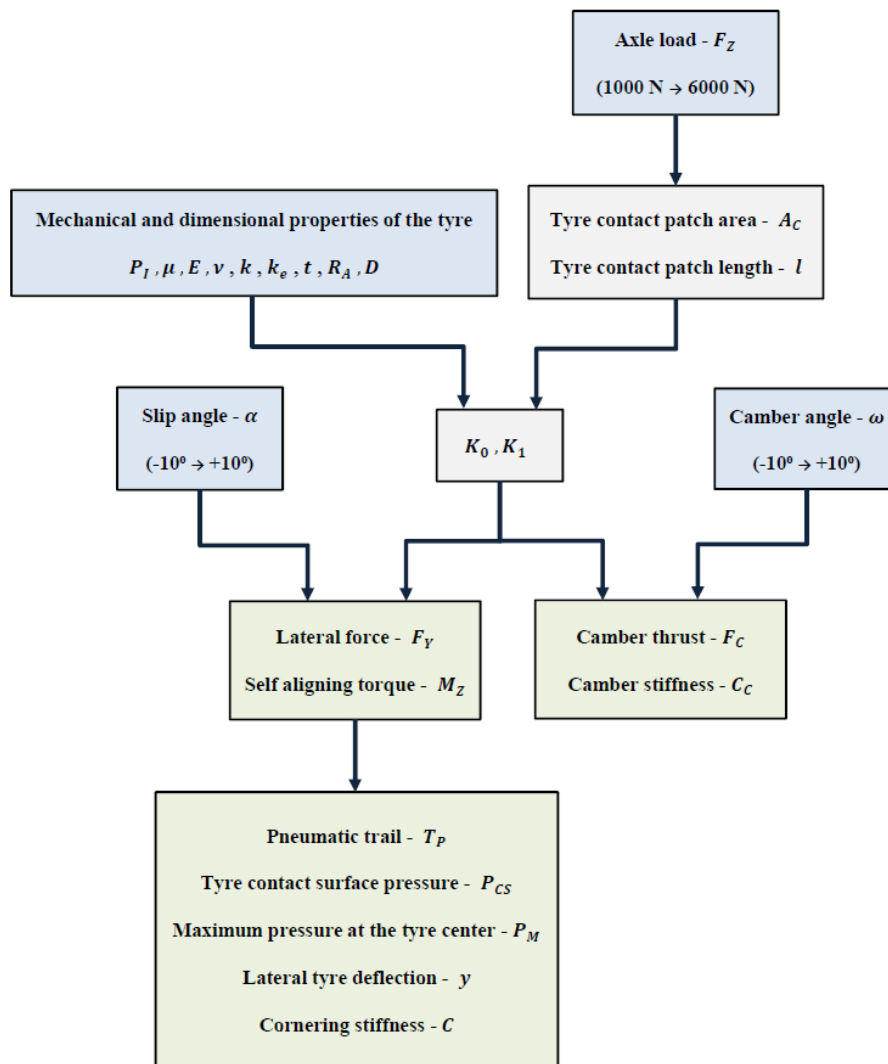


Figure 5. The flow chart of the mathematical model

The lateral force F_Y and the self-aligning torque M_Z are a function of the axle load F_Z and the slip angle α expressed as follows. In addition to the mechanical and dimensional properties of the tyre, the contact area length l and the friction coefficient of the ground μ also have a significant effect on these parameters.

$$\varphi = \frac{C \cdot \tan \alpha}{F_Z \cdot \mu} \tag{9}$$

$$F_Y = \mu \cdot F_Z \cdot \left(\varphi - \frac{1}{3} \cdot \varphi^2 + \frac{1}{27} \cdot \varphi^3 \right) \tag{10}$$

$$M_Z = \frac{\mu \cdot F_Z}{6} \cdot \left(\varphi - \varphi^2 + \frac{1}{3} \cdot \varphi^3 - \frac{1}{27} \cdot \varphi^4 \right) \tag{11}$$

The cornering stiffness value C , which provides an idea about the cornering ability of the vehicle, is expressed as the differentiation of the lateral force F_Y with respect to the slip angle α .

$$C = \frac{K_1 \cdot l^2}{2} = - \left. \frac{dF_Y}{d\alpha} \right|_{\alpha=0} \tag{12}$$

The pneumatic trail T_P is determined by the ratio of the self-aligning torque M_Z to the lateral force F_Y

$$T_P = \frac{M_Z}{F_Y} \tag{13}$$

The pressure distribution P_{CS} on the tyre contact area center axis, the maximum pressure value P_M , and the amount of tyre lateral deflection y are expressed as follows.

$$P_{CS} = 4 \cdot P_M \cdot \frac{x}{l} \cdot \left(1 - \frac{x}{l} \right) \tag{14}$$

$$P_M = \frac{3 \cdot F_Z}{2 \cdot A_C} \tag{15}$$

$$y = \frac{F_Y \cdot \beta^3 \cdot l^2}{2 \cdot k} \cdot \frac{x}{l} \cdot \left(1 - \frac{x}{l}\right) \tag{16}$$

The camber thrust F_C is directly affected by the mechanical and dimensional properties of the tyre, similar to the lateral force F_Y . It is also a function of camber angle ω and effective tyre radius R_0 [42].

$$F_C = \frac{K_1 \cdot l^3}{12 \cdot R_0} \cdot \omega \tag{17}$$

The effective tyre radius R_0 is expressed by the unloaded tyre radius R , the vertical force F_Z , and the longitudinal tyre spring constant k_e .

$$R_0 = R - \frac{F_Z}{k_e} \tag{18}$$

Finally, the camber stiffness C_c is defined as the differentiation of the camber thrust F_C with respect to the camber angle ω .

$$C_c = -\left. \frac{dF_C}{d\omega} \right|_{\omega=0} \tag{19}$$

4 RESULTS AND DISCUSSION

A sample of the relationship between lateral force and slip angle for an automobile, depending on the input parameters and the mathematical model, is shown in Figure 6. The amount of lateral force increased linearly at small slip angles for all axle load values. After the linear increase, the lateral force increase slowed down

and reached its peak. The peak of the curve obtained shows how much lateral force the tyre can produce with its mechanical and dimensional properties. After the peak, the lateral force decreases slightly and becomes satiated at large slip angles. When the effect of axle load on lateral force is examined, it is seen that the amount of lateral force increases in proportion to the increase in the axle load. As the amount of axle load increased, the lateral force variation due to the unit slip angle also increased, and the effect of the axle load was more evident at the satiation levels of the lateral force. It has been determined that the amount of lateral force reaches satiation at smaller slip angles with increasing axle load amount.

When the variation of the self-aligning torque depending on the slip angle is examined in Figure 7, a linear increase is observed similar to the lateral force graph for small slip angles. With increasing slip angle, the self-aligning torque also increased rapidly and reached a maximum at one point. It has been found that the maximum self-aligning torque is reached at smaller slip angles for large axle load values. As the axle load value decreased, the peak was observed at greater slip angles. After this peak, as the slip angle increases, the self-aligning torque value decreases and tends to be zero at large slip angles. It is seen that the effect of axle load on self-aligning torque is quite high at all slip angles. The main reason for this is that the tyre contact area length increases with increasing axle load, and therefore the amount of moment generated by the lateral force acting on the tyre also increases.

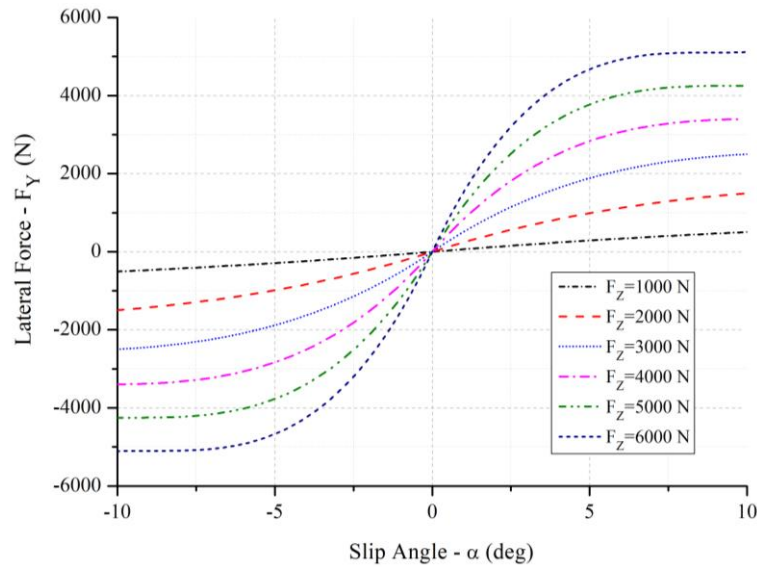


Figure 6. Slip angle versus lateral force for different vertical loads

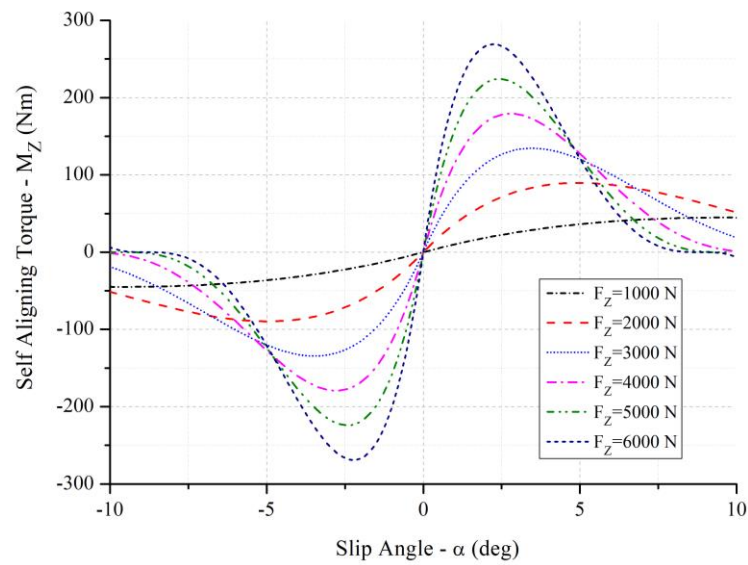


Figure 7. Slip angle versus self-aligning torque for different vertical loads

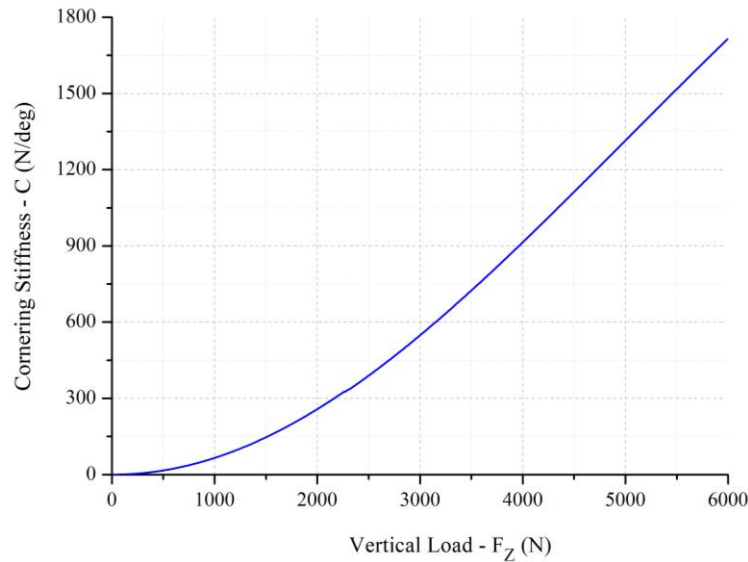


Figure 8. Cornering stiffness versus vertical load

The slope of the linear region seen at small slip angles in Figure 6 corresponds to the change in lateral force per unit slip angle of the tyre and is called the cornering stiffness. The lateral movement of a vehicle also takes place within this linear region which is usually seen at small slip angles. The cornering stiffness value is one of the significant parameters in interpreting the cornering ability of the vehicle. The change in cornering stiffness depending on the axle load is shown in Figure 8. Cornering stiffness increased exponentially up to an axle load of about 2000 N. However, it increased almost linearly at higher axle loads.

The distance between the point where the lateral force acts on the contact patch and the vertical tyre axis is the pneumatic trail. In other words, the pneumatic trail is the ratio of the lateral force to the self-aligning torque. As seen in Figure 9, it has been determined that the

pneumatic trail has a maximum value at 0° slip angle, decreases close to linear with increasing slip angle, and reaches zero. The increase in axle load caused the pneumatic trail to reach zero at larger slip angles. The reason for this can be considered as the self-aligning torque tends to zero at much smaller slip angles as the axle load value increases.

The tyre contact area pressure distribution, seen in Figure 10, expresses the pressure values acting on the tyre tread along the tyre contact area center axis and appears as an asymmetrical parabola. For all axle loads, the maximum pressure was determined to be approximately 210 kPa, and it occurred at the pneumatic trail points. The reason why the curves are asymmetrical is that the maximum pressure values occur at the pneumatic trail points. A balanced pressure drop across the contact area was observed on either side of the maximum pressure

Depending on the increasing axle load, the tyre contact area length increased, and the change in the pneumatic trail became more evident. It has been determined that the maximum pressure value in the tyre contact area center axis is not affected by the axle load. Figure 11 shows the amount of lateral deflection in the tyre contact area center axis along the tyre contact length. The lateral tyre deflection studied for a lateral force of 3000 N is obtained as an asymmetrical parabola as in the contact area pressure distribution. This is because the

deformation direction on the front of the tyre is almost parallel to the tyre's travel direction. Relatively no slippage is observed in this region. The actual slip is observed at the rear of the tyre contact surface and the greatest lateral deformation has occurred in this region. It has been determined that the amount of lateral tyre deflection also increases in direct proportion to the increasing contact length depending on the amount of axle load.

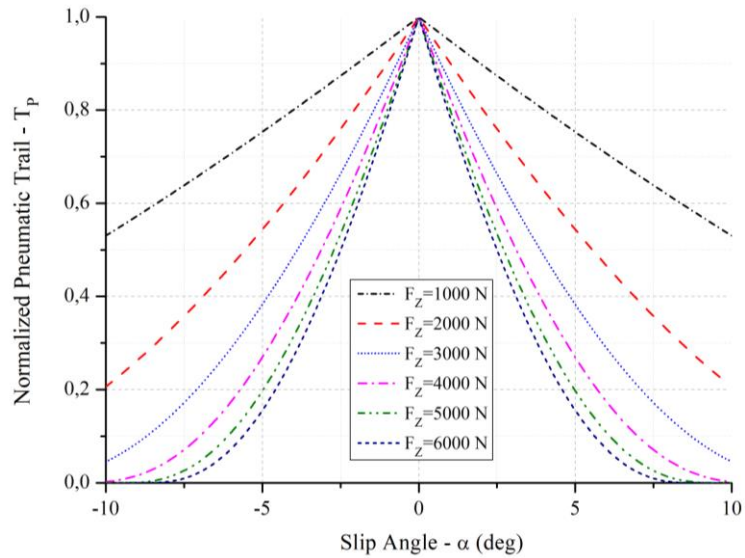


Figure 9. Normalized pneumatic trail versus slip angle for different vertical loads

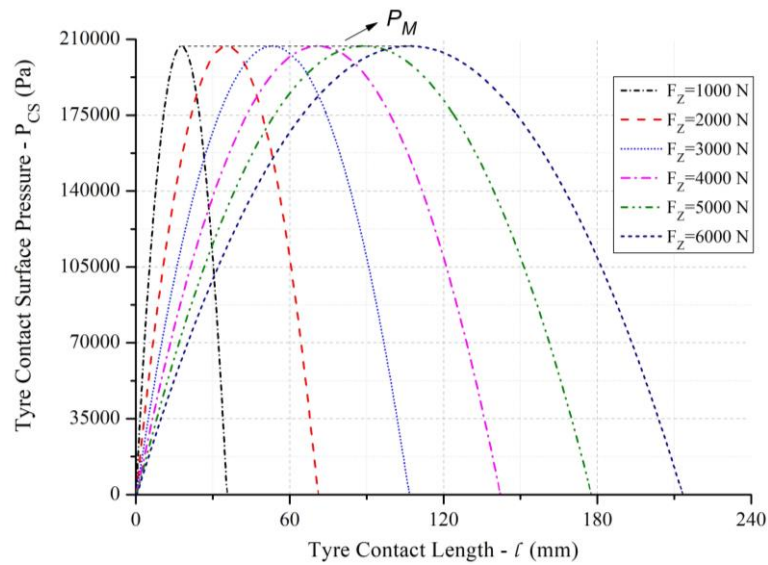


Figure 10. Tyre contact surface pressure versus tyre contact length for different vertical loads

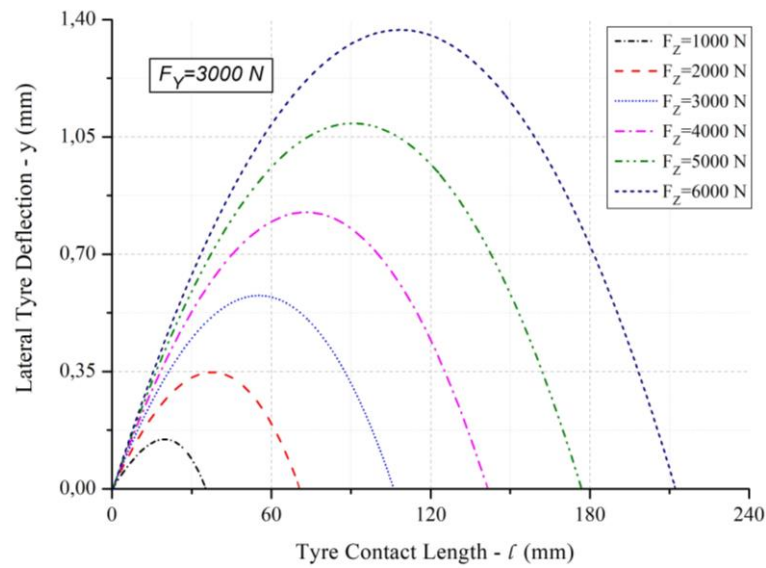


Figure 11. Lateral tyre deflection versus tyre contact length for different vertical loads

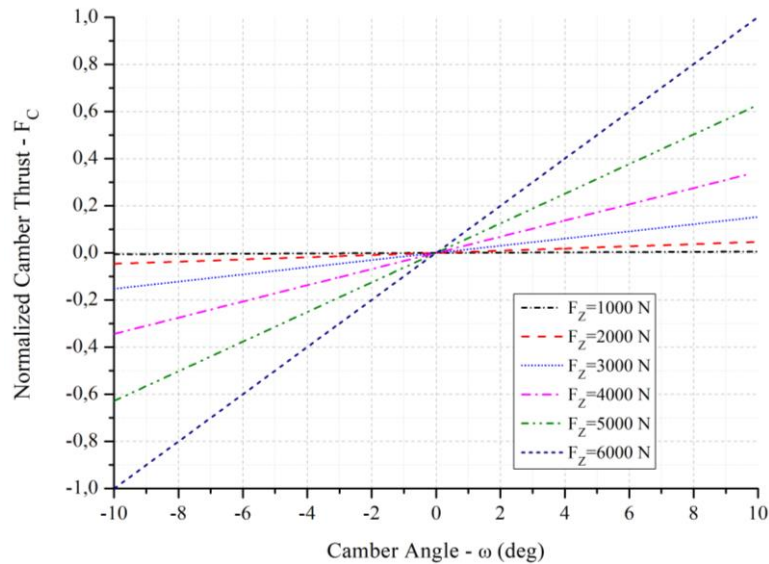


Figure 12. Normalized camber thrust versus camber angle for different vertical loads

Figure 12 shows the change in camber thrust depending on the camber angle. Here the slip angle is zero. It has been determined that the camber thrust increases with increasing camber angle, almost linearly. On the other hand, the increase of axle load, increased the change in camber thrust per unit camber angle.

As seen in Figure 13, camber stiffness which is the change in camber thrust per unit camber angle of the wheel increased almost linearly with increasing axle

load. The camber stiffness value gives information about the current camber angle of the wheel and how it responds to the change in camber angle. It can be said that camber stiffness has similar properties to cornering stiffness. While the increase in the camber stiffness at low axle loads was quite small, the increase in the camber stiffness with the increase in the axle load also reached very high levels.

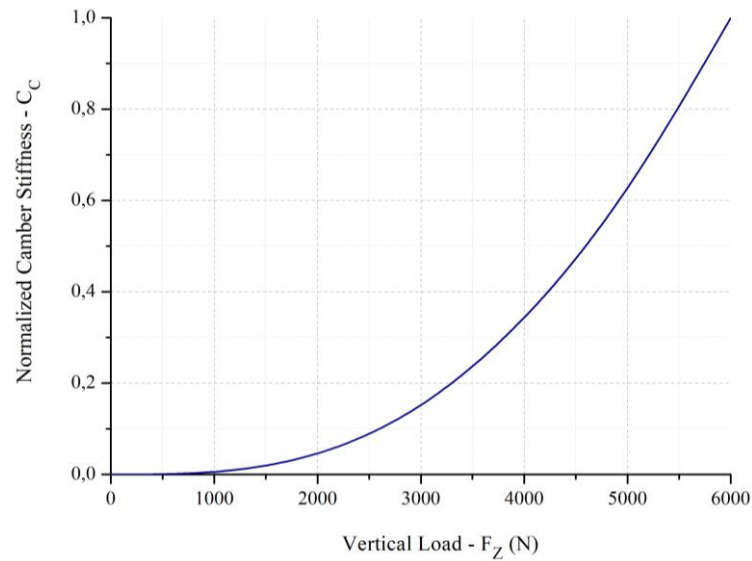


Figure 13. Normalized camber stiffness versus vertical load

5. CONCLUSIONS

In this study, the effects of axle load on slip angle were investigated. For this purpose, different parameters affecting tyre mechanics are handled according to axle load. First, the variation of the lateral force and self-aligning torque with the slip angle was determined. Then, using these parameters, pneumatic trail, tyre contact area pressure distribution, tyre contact area maximum pressure value, lateral tyre deflection, and cornering stiffness were calculated. Additionally, the camber thrust and camber stiffness values were investigated independently of the slip angle. It was observed that the amount of lateral force increased in proportion to the change in axle load. The effect of the axle load was more evident at the saturation levels of the lateral force. The maximum self-aligning torque is achieved at small slip angles for large axle load values. It has been determined that the effect of axle load on self-aligning torque is quite high at all slip angles. The cornering stiffness progressed at a low rate of increase up to certain axle loads. It showed an almost linear increase at large axle loads. The increase in axle load caused the pneumatic trail to reach zero at larger slip angles. For all axle loads, the maximum pressure was determined to be approximately 210 kPa and occurred at the pneumatic trail points. It has been determined that the maximum pressure value in the tyre contact area center axis is not affected by the axle load. The lateral tyre deflection examined for a lateral force of 3000 N was obtained as an asymmetrical parabola as in the pressure distribution of the contact area. It has been observed that the lateral deflection of the tyre changes in direct proportion with the increase in the contact area length caused by the increasing axle load. It was seen that the camber thrust increased proportionally with the camber angle, and the increase in the axle load increased the change in camber thrust per unit camber angle. Finally, while the increase in camber stiffness at low axle

loads was quite small, the increase in camber stiffness with the increase in axle load reached very high levels.

DECLARATION OF ETHICAL STANDARDS

The authors of this article declare that the materials and methods used in this study do not require ethical committee permission and/or legal-special permission.

AUTHORS' CONTRIBUTIONS

Turan Alp Arslan: Conceptualization, Methodology, Software, Writing – review & editing original draft.

İbrahim Çelik: Conceptualization, Methodology, Software, Writing – review & editing original draft.

Faruk Emre Aysal: Conceptualization, Methodology, Writing – review & editing original draft.

Hüseyin Bayrakçeken: Methodology, review & editing original draft

CONFLICT OF INTEREST

There is no conflict of interest in this study.

NOMENCLATURE

A_C	tyre contact area (m ²)
ABS	Anti-lock Braking System
b	contact width (m)
C	cornering stiffness (N/deg)
C_C	camber stiffness (N/deg)
d	tyre sidewall height during deformation (m)
D	rim diameter (inch)
E	Young's modulus of the tread material (Pa)
ESC	Electronic Stability Control

F_C	camber thrust (N)
F_Y	lateral force (N)
F_Z	vertical force (N)
FEM	Finite Element Method
G	shear modulus of the tread (Pa)
GNSS	Global Navigation Satellite Systems
GPS	Global Positioning System
h	tyre sidewall height (m)
I	moment of inertia of area of the contact (m ⁴)
IMU	Inertial Mobility Units
INS	Inertial Navigation System
k	spring constant per unit length of the spring support (N/m)
k_e	longitudinal spring constant of the tyre (N/m)
l	tyre contact length (m)
M_Y	wheel torque (Nm)
M_Z	self-aligning torque (Nm)
P_{CS}	tyre contact surface pressure (Pa)
P_I	tyre inflation pressure (Pa)
P_M	maximum pressure at the tyre center (Pa)
R	unload tyre radius (m)
R_0	effective tyre radius (m)
R_A	tyre aspect ratio
t	tyre width (m)
T_P	pneumatic trail (m)
TCS	Traction Control System
y	lateral tyre deflection (m)
x	distance in tyre rotation axis (m)
α	slip angle (deg)
μ	friction coefficient
ν	poisson ratio of the tread
ω	camber angle (deg)

REFERENCES

- [1] World Health Organization, "Global status report on road safety 2018", Geneva, Switzerland, (2018).
- [2] Chang F.R., Huang H.L., Schwebel D.C., Chan A.H. and Hu G.Q., "Global road traffic injury statistics: Challenges, mechanisms and solutions", **Chinese Journal of Traumatology**, 23(4):216-218, (2020).
- [3] World Health Organization, "Global plan for the decade of action for road safety 2011-2020", Geneva, Switzerland, (2011).
- [4] The United Nations, "Sustainable development goal 3, ensure healthy lives and promote well-being for all at all ages", (2019).
- [5] Huang H., Yin Q., Schwebel D.C., Ning P. and Hu G., "Availability and consistency of health and non-health data for road traffic fatality: Analysis of data from 195 countries, 1985-2013", **Accident Analysis and Prevention**, 108:220-226, (2017).
- [6] Kuşkan E. and Çodur M.Y., "Performance analysis of multilayer perceptron, regression and nearest neighbor algorithms in classification of traffic accidents", **Journal of Polytechnic**, 25(1):373-380, (2022).
- [7] Hsu Y.H.J., Laws S.M. and Gerdes J.C., "Estimation of tire slip angle and friction limits using steering torque", **IEEE Transactions on Control Systems Technology**, 18(4):896-907, (2010).
- [8] Bengler K., Dietmayer K., Farber B., Maurer M., Stiller C. and Winner H., "Three decades of driver assistance systems: Review and future perspectives", **IEEE Intelligent Transportation Systems**, 6(4):6-22, (2014).
- [9] Lu M., "Modelling the effects of road traffic safety measures", **Accident Analysis & Prevention**, 38(3):507-517, (2006).
- [10] Winner V.H., Hakuli S., Lotz F. and Singer C., "Handbuch Fahrer-assistenzsysteme", 3rd ed., **Springer Vieweg**, ISBN-13: 978-3-658-05733-6, Berlin, Germany, (2015).
- [11] Aga M. and Okada A., "Analysis of vehicle stability control (VSC)'s effectiveness from accident data", **In: Proceedings of 18th International Technical Conference on the Enhanced Safety of Vehicles**, Nagoya, Japan, Paper no. 541, (2003).
- [12] Sferco R., Page Y., Coz J.Y.L. and Fay P.A., "Potential effectiveness of the electronic stability programs (ESP)-What European field studies tell us", **In: Proceedings of 17th International Technical Conference on the Enhanced Safety of Vehicles**, Amsterdam, Netherlands, Paper no. 2001-S2-O-327, (2001).
- [13] Zanten A.T., Erhardt R. and Pfaff G., "VDC, the vehicle dynamics control system of Bosch", **SAE Transactions**, 104(6):1419-1436, (1995).
- [14] Kiencke U. and Daiß A., "Observation of lateral vehicle dynamics", **Control Engineering Practice**, 5(8):1145-1150, (1997).
- [15] Fukada Y., "Estimation of vehicle slip-angle with combination method of model observer and direct integration" **In: Proceedings of 4th International Symposium Advance Vehicle Control**, Nagoya, Japan, Paper no. 9836626, 201-206, (1998).
- [16] Venhovens P.J.T. and Naab K., "Vehicle dynamics estimation using Kalman filters", **Vehicle System Dynamics**, 32(2-3):171-184, (1999).
- [17] Stephant J., Charara A. and Meizel D., "Virtual sensor: Application to vehicle sideslip angle and transversal forces", **IEEE Transactions Industrial Electronics**, 51(2):278-289, (2004).
- [18] Hahn J.O., Rajamani R. and Alexander L., "GPS-based real-time identification of tire-road friction coefficient", **IEEE Transactions on Control Systems Technology**, 10(3):331-342, (2002).
- [19] Yasui Y., Tanaka W., Muragishi Y., Ono E., Momiyama M., Katoh H., Aizawa H. and Imoto Y., "Estimation of lateral grip margin based on self-aligning torque for vehicle dynamics enhancement", **SAE Transactions**, 113(6):632-637, (2004).
- [20] Iijima T., Raksincharoensak P., Michitsuji Y. and Nagai M., "Vehicle side slip angle estimation methodology using a drive recorder", **Journal of Vibration and Control**, 16(4):571-583, (2010).
- [21] Behroozinia P., Khaleghian S., Taheri S. and Mirzaeifar R., "An investigation towards intelligent tyres using finite element analysis", **International Journal of Pavement Engineering**, 21(3):311-321, (2020).
- [22] Cho K., Son H., Wang Y., Nam K. and Choi S., "Vehicle side-slip angle estimation of ground vehicles based on a lateral acceleration compensation", **IEEE Access**, 8:180433-180443, (2020).

- [23] Çelik İ. and Sonugür G., “The test of electric vehicle with electronic differential system in different road conditions”, **Journal of Polytechnic**, 25(3):1021-1030, (2022).
- [24] Han Y., Lu Y., Chen N. and Wang H., “Research on the identification of tyre-road peak friction coefficient under full slip rate range based on normalized tyre model”, **Actuators**, 11(59):1-17, (2022).
- [25] Lee H. and Choi S., “Development of collision avoidance system in slippery road conditions”, **IEEE Transactions on Intelligent Transportation Systems**, doi: 10.1109/TITS.2022.3168668, (2022).
- [26] Ryu J., Rossetter E.J. and Gerdes J.C., “Vehicle sideslip and roll parameter estimation using GPS”, **In: Proceedings of 6th International Symposium on Advanced Vehicle Control**, Hiroshima, Japan, 373-380, (2002).
- [27] Baffet G., Charara A. and Lechner D., “Estimation of vehicle sideslip, tire force and wheel cornering stiffness”, **Control Engineering Practice**, 17(11):1255-1264, (2009).
- [28] Daily R. and Bevly D.M., “The use of GPS for vehicle stability control systems”, **IEEE Transactions on Industrial Electronics**, 51(2):270-277, (2004).
- [29] Ryu J. and Gerdes J.C., “Integrating inertial sensors with GPS for vehicle dynamics control”, **Journal of Dynamic Systems, Measurement, and Control**, 126(2)-243-254, (2004).
- [30] Piyabongkarn D., Rajamani R., Grogg J.A. and Lew J.Y., “Development and experimental evaluation of a slip angle estimator for vehicle stability control”, **IEEE Transactions on Control Systems Technology**, 17(1)-78-88, (2009).
- [31] Grip H.F., Imsland L., Johansen T.A., Kalkkuhl J.C. and Suissa A., “Vehicle sideslip estimation: Design, implementation, and experimental validation”, **IEEE Control Systems**, 29(5): 36-52, (2009).
- [32] Ray L.R., “Nonlinear estimation of vehicle state and tire forces”, **In: 1992 American Control Conference**, Chicago, USA, 526-530, (1992).
- [33] Ray L.R., “Nonlinear state and tire force estimation for advanced vehicle control”, **IEEE Transactions on Control Systems Technology**, 3(1):117-124, (1995).
- [34] Ray L.R., “Nonlinear tire force estimation and road friction identification: Simulation and experiments”, **Automatica**, 33(10):1819-1833, (1997).
- [35] Cheli F., Sabbioni E., Pesce M. and Melzi S., “A methodology for vehicle sideslip angle identification: Comparison with experimental data”, **International Journal of Vehicle Mechanics and Mobility**, 45(6):549-563, (2007).
- [36] You S.H., Hahn J.O. and Lee H., “New adaptive approaches to real-time estimation of vehicle sideslip angle”, **Control Engineering Practice**, 17(12):1367-1379, (2009).
- [37] Stéphant J., Charara A. and Meizel D., “Evaluation of a sliding mode observer for vehicle sideslip angle”, **Control Engineering Practice**, 15(7):803-812, (2007).
- [38] Kim H.H. and Ryu J., “Sideslip angle estimation considering short-duration longitudinal velocity variation”, **International Journal of Automotive Technology**, 12(4):545-553, (2011).
- [39] Pi D.W., Chen N., Wang J.X. and Zhang B.J., “Design and evaluation of sideslip angle observer for vehicle stability control”, **International Journal of Automotive Technology**, 12(3):391-399, (2011).
- [40] Köylü H., “Improvement of dynamic wheel load oscillations by coupling pitch motion into bounce motion during pitching motion of passenger vehicle”, **Journal of Polytechnic**, 24(4):1473-1489, (2021).
- [41] Chatur S., “Computer based wireless automobile wheel alignment system using accelerometer”, **The International Journal of Engineering And Science**, 4(9):62-69, (2015).
- [42] Abe M., “Vehicle handling dynamics, theory and application”, 1nd ed., **Butterworth-Heinemann**, ISBN-13: 978-1-8561-7749-8, Oxford, UK, (2009).
- [43] Çetinkaya S., “Taşıt mekaniği”, 8th ed., **Nobel Akademik Yayıncılık**, ISBN: 978-605-133-463-9, Ankara, Turkey, (2017).
- [44] Gent A.N. and Walter J.D., “The pneumatic tire”, 1nd ed., **National Highway Traffic Safety Administration**, DOT HS 810 561, Washington, USA, (2006).
- [45] Smith N.D., “Understanding parameters influencing tire modeling”, **In: Formula SAE Platform**, Fort Collins, USA, (2004).
- [46] Milliken W.F. and Milliken D.L., “Race car vehicle dynamics”, 5th ed., **SAE Publications**, ISBN1-56091-526-9, Allegheny, USA, (1995).
- [47] Kavitha C., Shankar S.A., Karthika K., Ashok B. and Ashok S.D., “Active camber and toe control strategy for the double wishbone suspension system”, **Journal of King Saud University – Engineering Sciences**, 31(4):375-384, (2019).
- [48] Balkwill J., “Performance vehicle dynamics, engineering and applications”, 1nd ed., **Butterworth-Heinemann**, ISBN: 978-0-12-812693-6, Oxford, UK, (2018).
- [49] Blundell M. and Harty D., “The multibody systems approach to vehicle dynamics”, 1nd ed., **Butterworth-Heinemann**, ISBN: 978-0-08-099425-3, Oxford, UK, (2004).
- [50] Mitsuhashi Y. and Fujii S., “Validation of Fiala model for motorcycle with FEM tire model”, **Transactions of Society of Automotive Engineers of Japan**, 44(1):75-80, (2013).
- [51] Fiala E., “Seitenkräfte am rollenden Luftreifen”, **VDI-Zeitschrift**, 96:973-979, (1954).
- [52] Babulal Y., Stallmann M.J. and Els P.S., “Parameterisation and modelling of large off-road tyres for on-road handling analyses”, **Journal of Terramechanics**, 61:77-85, (2015).
- [53] Ünker F., “Angular momentum control for preventing rollover of a heavy vehicle”, **International Journal of Automotive Science and Technology**, 6(2):135-140, (2022).
- [54] Eroğlu M., Koç M. A., Kozan R. and Esen İ., “Comparative analysis of full car model with driver using PID and LQR controllers”, **International Journal of Automotive Science and Technology**, 6(2):178-188, (2022).
- [55] Kageyama I. and Kuwahara S., “A study on tire modeling for camber thrust and camber torque”, **JSAE Review**, 23(3):325-331, (2002)